

Sources of organic detritus under mussel farms in the Ría de Ares-Betanzos

JOERI KAAL¹ AND CSIC-PROINSA MUSSEL LAB TEAM²

¹Pyrolyscience, Santiago de Compostela, Spain

²Instituto de Investigaciones Marinas, CSIC, Vigo, Spain/Grupo Proinsa, Sada, Spain

Compiled September 13, 2018

The Galician coastline is enormously productive of high-quality seafood due to the vast supply of nutrients, oxygen and plankton in this unique coastal upwelling system¹. One of the characteristics of the Rías is the abundance of raft farms, “bateas”: floating wooden structures with 500 ropes hanging into the water column and on which mussels grow (suspended mussel farming). Galician mussel farms represent the highest mussel (*Mytilus galloprovincialis*) producing area in Europe (>250 Million kg per year)². These farms are known to both boost biodiversity in the water column, providing refuge to fauna and anchoring for macroalgae, but also to cause alteration of benthic communities due to the massive production of “biodeposits” (mussel fall-out and faeces), sometimes resulting into anoxia at the seabed^{3,4}. The Marine Research Institute (IIM) of the Spanish Research Council (CSIC) has been studying the ecology, chemistry and sustainability of these suspended bivalve systems for many years^{2,5}. Now, an effort has been made to identify the potential of analytical pyrolysis techniques to provide information on biodeposit composition by means of analysis of particulate organic matter (POM) from sediment traps deployed underneath the farms.

1. MATERIALS AND METHODS

The samples were obtained from a mussel culture polygon in the vicinities of Lorbé in the Ría de Ares-Betanzos (Sada, A Coruña province, Galicia, NW Spain), consisting of 107 rafts and an annual production of 10,000 tons of mussels. The particulate organic matter (POM) samples were obtained from multitrap collectors that were deployed beneath raft #46 (further from coast, 16 m water depth) and raft #14 (closer to coast and fish cages, 14 m depth) (Figure 1) on the 2nd and 3rd of May, 2011 (Spring bloom oceanographic scenario⁵). Samplers were deployed at the bow (or proa, i.e. water entry) and stern (popa, water exit) sides of the rafts. The traps contained four collectors which were open for no more than 12 h to mitigate the influence of microbial decomposition in the traps. Two of the 4 collectors within each trap were analyzed, T1 and T2 (these correspond to adjacent

PVC cylinders within the multitrap). No preservatives were used (for details, see Zúñiga et al. 2014⁵). Hence, a total of 8 samples were considered (2 rafts x 2 positions x 2 replicates) as a first approach to determine biodeposit sources and identify mechanisms that control variability in POM's molecular composition. After retrieving the suspensions from the traps their content was filtered through Whatman GF/F filters (0.7 μ m pore size). Due to the low inorganic matter content of these samples (< 10%), no sample treatment other than drying at 100 °C, was performed (it would be a different scenario for the samples from Winter, which may have inorganic contents exceeding 75%)⁵.

The Py-GC-MS analyses were performed by inserting solid POM (that was scraped directly from the filters) into quartz tubes with quartz wool on both ends. Pyrolysis was performed for 10 s at 650 °C, with a Pyroprobe 5000. The pyrolyzer was connected to a 6890 GC and 5975 MSD from Agilent Technologies. For chromatographic temperature profiles and MSD parameters, see kaal et al.⁶. Major peaks were quantified on the basis of characteristic *m/z* fragments. Data evaluation was based on i) pyrolysis compound percentages, analysis of variance (one-way ANOVA) and linear correlation analysis.

Table 1 presents the list of samples analyzed and parameters that are used for comparison with the Py-GC-MS data: fluxes of nitrogen (N_{total}), carbon (C_{total}) and organic C (C_{org}), which is modified data after Zúñiga et al. (2014)⁵.

2. RESULTS AND DISCUSSION

A large array of carbohydrate- and especially protein-derived pyrolysis products were detected (pyrroles, pyridines, diketodipyrrole, indoles) (Table 2, see end of document). They include markers of *N*-acetylglucosamine polymers (acetamidoglycans), which can be found in chitin from arthropod/crustacean/mollusk exoskeletons (and squid beaks), bacterial cell wall material, and the mucus of mollusks that cover faeces and pseudofaeces (Figure 2). The majority, if not all, of the other carbohydrate and protein products probably originate from mussel derivatives or marine biota such as phytoplankton.

The most abundant group of products are the N-containing compounds, which account for 27.4 ± 3.1 % of TQPA (percentage of total quantified peak area), followed by monocyclic aromatic hydrocarbons (MAHs; 23.1 ± 3.7 %) and phenols (22.8 ± 5.1 %).

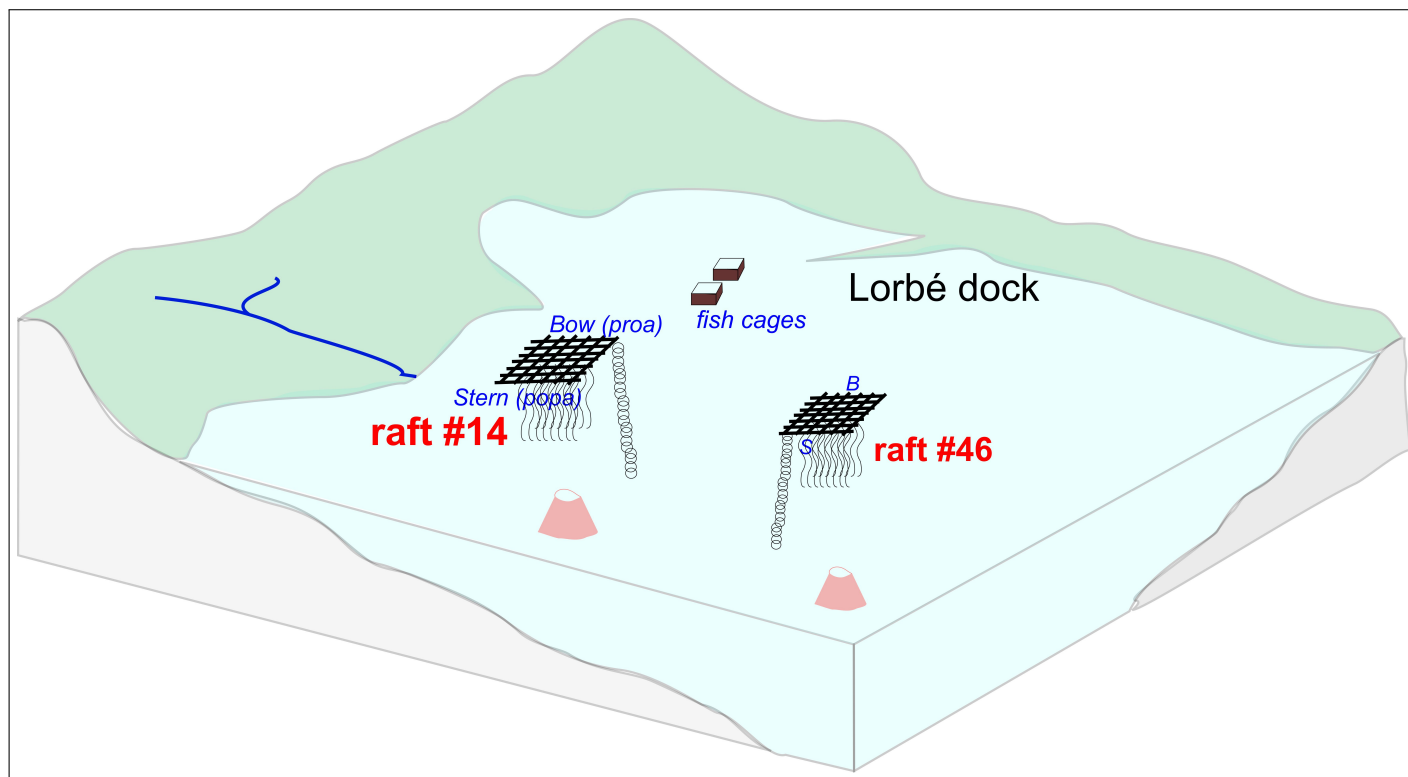


Fig. 1. Schematic representation of the analyzed system, showing the mussel cultures (rafts) and underlying sediment traps.

This set of compounds is a clear indication that the POM originates from predominantly N-rich sources. The abundance of not only many protein markers (such as indoles from tryptophan or diketopiperazines from dimerization reactions of peptide chains during pyrolysis) but also products *N*-acetylglucosamine biopolymers suggests that mussel detritus, whether it be chitin from shells or mucus in faeces droppings, is a significant, if not dominant source of POM. Note that theoretically pseudofaeces (droppings of mucus-entangled inorganic matter filtered by the animal but which did not pass its digestive system) may also provide mucus to the biodeposits but due to the low seston concentration in the clear waters of NW Spain in general, production of pseudofaeces is unlikely (seston below threshold of 4 mg/L)⁵.

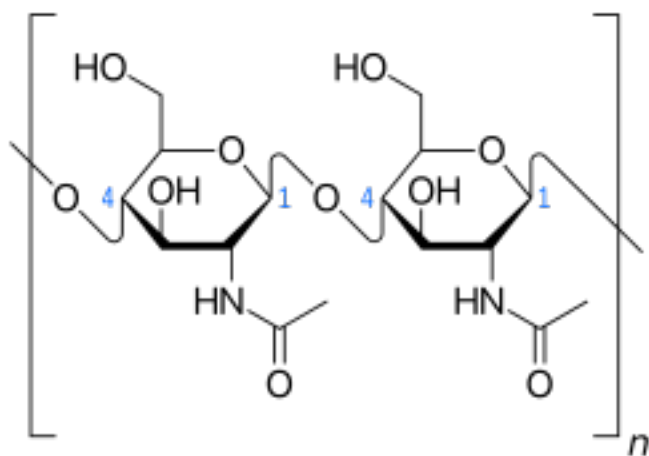


Fig. 2. Basic structure of *N*-acetylglucosamine polymers in mucus or chitin (not representative for peptidoglycan).

The proteins may originate from a combination of the mussel's faeces and alternative (marine) sources such as macroalgae and plankton. According to the high chlorophyll *a* content of these samples⁵, detritus from primary production is expected to be significant. The phenols may largely originate from aromatic amino acids in proteins such as tyrosine moieties, and the same can be argued for toluene among the MAH which is associated with phenylalanine⁷. Another component of the POM is of pyrogenic origin: products of e.g. charcoal from wildfires or soot from incomplete fuel combustion. This pyrogenic POM is reflected by PAHs (1.6 ± 0.4 % naphthalene, alkylnaphthalenes, fluorene, biphenyl, phenylanthracene, etc.), but also benzene (MAH) and benzonitrile⁶ (N-containing pyrogenic POM). This reaffirms previous indications⁵ of the presence of a minor fraction of allochthonous POM from runoff, with a high C/N ratio, and which is concentrated in the littoral areas in the studied ría⁸. One sample produced a significant amount of a 5-methylbromindole (sample 20, Table 1), whereas

Table 1. List of samples analyzed and selected parameters

Raft	Date	Sampler	Sample	N _{total}	C _{total}	C _{org}
-	m/d/yr	-	-	mg/m ² d	mg/m ² d	mg/m ² d
P46 bow	5/2/2011	T1	17	405	2503	1603
P46 bow	5/2/2011	T2	18	304	1866	2092
P46 stern	5/2/2011	T1	19	813	5017	5101
P46 stern	5/2/2011	T2	20	619	4340	2833
P14 bow	5/3/2011	T1	27	186	1283	1045
P14 bow	5/3/2011	T2	28	210	1409	1321
P14 stern	5/3/2011	T1	29	447	3157	1958
P14 stern	5/3/2011	T2	30	488	3576	1930

the pyrolyzates of the other samples contained trace amounts of this molecule. This may be a natural organobromine compound from marine biota⁹, or a secondary pyrolysis reaction between inorganic bromine and protein-derived indole, and has not been detected previously identified in POM pyrolyzates. Methyl-bromide (MeBr) is also abundant.

The long-chain aliphatic products ($8.9 \pm 1.9\%$), or methylene chain compounds (MCC), also have various potential sources. Two phytadienes were detected among the MCC, which are probably products of chlorophyll, from phytoplankton and/or macroalgae. The remaining products, notably fatty acids, may originate from any source but especially algae and mussel faeces were expected to be prolific of these compounds. Carbohydrate products account for $8.7 \pm 2.3\%$. They may be of any biological source mentioned above, but the high abundance of *N*-acetylglucosamine polysaccharide products among the *N*-compounds suggests that the carbohydrates may originate predominantly from chitin and/or mucus. Contamination indicators ($4.9 \pm 4.7\%$) are *tert*-phenols and a bisphenol product. They probably both originate from bisphenol-type anthropogenic contamination. The C_{3,1}-phenol compound shows similar differences in proportion among samples, and is therefore likely to originate from such contamination as well. Finally, lignin from terrestrial plants could not be unequivocally identified but the presence of a compound with *m/z* 120 and 91 at the expected retention time of 4-vinylphenol might reflect traces of land plant debris (if so, probably sedges or grasses including seagrasses).

For the ANOVA, we used all continuous variables as input attributes and the discrete parameters raft number (raft #46 vs. raft #14), trap position (bow vs. stern), and sampler (T1 vs. T2) as target variables.

As expected, none of the variables is affected by sampler number (T1/T2) located at the same spot (different cylinders in the same trap). For trap position, some significant ($P < 0.05$) differences were observed. Firstly, the fluxes of C_{total} and N_{total} were higher in the trap deployed at the stern position (popa). This suggests that the waters that flow through the rafts and the mussel cords gain in POM content along this path through the raft and illustrate biodeposition intensity differences. In other words, the effects of the rafts on the deposition of faeces can be observed not only from mass fluxes but also from relative contributions to POM. Among the Py-GC-MS products, stern samples are enriched in 3-acetamidopyrone (mussel chitin/mucus) and levoglucosan (chitin and perhaps other polysaccharides). Bow

samples are enriched in MeBr. All the other >60 variables did not show significant differences.

For raft location, #14 was enriched in benzene, benzonitrile and fluorene (black-carbon derived) whereas #46 is enriched in some aliphatic products (an alkane/alkene pair and C₁₆-alkylamide). This suggests that the site that is closer to the coastline is enriched in terrestrial black carbon materials, possibly indicative of fluxes of charcoal particles from rivers and streams that discharge in the area.

The linear correlations between the C and N fluxes showed some interesting relationships. Strong positive correlations between C_{total} and 3-acetamidopyrone ($r=0.92!$, $P < 0.005$), C₁-indole, diketopiperazines, levoglucosan and C₁₆-fatty acid probably show the effect of POM sedimentation rate and proportions of mucus (delivering the *N*-acetylglucosamine polymer) and phytoplankton (delivering protein). Negative correlations between C_{total} and MeBr, styrene and bisphenol products probably represents a dilution effect (less biodeposits: more background signal). The same patterns are observed for C_{org} and N_{total}. The C/N ratio is not correlated to any pyrolysis product.

3. CONCLUSIONS

The molecular properties of the POM could be largely traced back to nitrogen-containing biopolymers, in particular protein and mucus/chitin. Mucus and chitin cannot be distinguished on the basis of the available data yet, as we have not analyzed reference materials for mussel mucus. The chitin/mucus originates predominantly from the mussel particles that trickle down from the rafts into the traps, possibly representing fall-off (although unlikely) and, most importantly, faeces. The protein originates from mussel debris (mucus/chitin) and plankton, and the presence of phytadienes provide strong evidence for algae-derived aliphatic POM (chlorophyll). The relative proportions of mucus/chitin and phytoplanktonic protein and aliphatic POM cannot be addressed: pyrolytic reactions are complex and chitin is entangled in protein which is difficult to distinguish from non-entangled protein in phytoplankton. However, from the ANOVA it was concluded that mussel debris was more abundant in the exit (stern) than entry (bow) of the mussel farms, which may reflect the background signal of POM from sources that are not directly associated to the bivalve cultures such as plankton. Other materials that were identified were traces of bisphenol contamination of unknown origin and fire residues

(charcoal, black carbon), the latter of which had a stronger signal in the pyrolysis chromatograms from the raft that was closest to the coastline (#14). In this context, it is worthy to mention that the region is subjected to a very intense fire regime. There is a clear potential of molecular characterization of particulate debris underneath mussel rafts to understand organic matter cycling and seafloor ecology.

ACKNOWLEDGEMENTS The efforts of Uxío Labarta, María-José Fernández-Reiriz, Diana Zúñiga and Carmen González Castro, among other members of the CSIC-PROINSA Mussel Farm Team, allowed for the materialization of this collaboration.

4. REFERENCES

1. Fraga, F., 1981. Upwelling off the Galician Coast, North-west Spain. Book Series: Coastal and Estuarine Sciences, Volume 1: 176-182. <https://doi.org/10.1029/CO001p0176>.
2. Labarta, U., Fernández-Reiriz, M.J., Pérez-Camacho, A., Pérez-Corbacho, E., 2004. El mejillón, un paradigma bioeconómico. In: Fundación Caixa Galicia (Ed.), Bateiros, mar, mejillón. Una perspectiva bioeconómica: Centro de Investigación Económica y Financiera. Editorial Galaxia, Vigo, pp. 19-47.
3. Otero, X.L., Calvo de Anta, R.M., Macías, F., 2008. Iron geochemistry under mussel rafts in the Galician ria system (Galicia-NW Spain). *Estuarine and Coastal Shelf Science* 81, 83-93.
4. Chamberlain, J., Fernandes, T.F., Read, P., Nickell, T.D., Davies, I.M., 2001. Impacts of biodeposits from suspended mussel (*Mytilus edulis* L.) culture on the surrounding surficial sediments. *ICES Journal of Marine Science*, 58: 411-416, doi:10.1006/jmsc.2000.1037.
5. Zúñiga, D., Castro, C.G., Aguiar, E., Labarta, U., Figueiras, F.G., Fernández-Reiriz, M.J., 2014. Biodeposit contribution to natural sedimentation in a suspended *Mytilus galloprovincialis* Lmk mussel farm in a Galician Ría (NW Iberian Peninsula). *Aquaculture* 432, 311-320.
6. Kaal, J., Martínez Cortizas, A., Nierop, K.G.J., Buurman, P., 2008. A detailed pyrolysis-GC/MS analysis of a black carbon-rich acidic colluvial soil (Atlantic ranker) from NW Spain. *Applied Geochemistry* 23, 2395-2405.
7. Tsuge, S., Matsubara, H., 1985. High-resolution pyrolysis-gas chromatography of proteins and related materials. *Journal of Analytical and Applied Pyrolysis* 8: 49-64.
8. Sánchez-Mata, A., Glémarec, M., Mora, J., 1999. Physico-chemical structure of the benthic environment of a Galician ría (Ría de Ares-Betanzos, north-west Spain). *Journal of the Marine Biological Association of the United Kingdom* 79, 1-21.
9. Andreotti, A., Bonaduce, I., Colombini, M.P., Ribechini, E., 2004. Characterisation of natural indigo and shellfish purple by mass spectrometric techniques. *Rapid Communications in Mass Spectrometry* 18: 1213-1220.

Table 2. List of pyrolysis products and source allocation (CARB=carbohydrate, LIG=lignin, MAH=monocyclic aromatic hydrocarbon, MCC=methylene chain compound, NCOMP=N-compound, PAH=polycyclic aromatic hydrocarbon, PHEN=phenol)

Label	RT (min)	Compound	m/z	group
1	1.075	MeBr	94+96	other
2	1.371	benzene	78	MAH
3	1.569	pyridine	79+52	NCOMP
4	1.601	pyrrole	67	NCOMP
5	1.704	toluene	91+92	MAH
6	1.780	acetamide	59	NCOMP
7	1.897	3/2-furaldehyde	95+96	CARB
8	2.037	C ₁ -pyrrole	80+81	NCOMP
9	2.146	C ₁ -pyridine	93+66	NCOMP
10	2.396	styrene	104+78	MAH
11	2.786	5-methyl-2-furaldehyde	110+109	CARB
12	2.942	benzonitrile	103+76	NCOMP
13	3.082	phenol	94+66	PHEN
14	3.701	C ₁ -phenol	107+108	PHEN
15	3.888	C ₁ -phenol	107+108	PHEN
16	4.075	carbohydrate compound	126	CARB
17	4.569	C ₂ -phenol	107+122	PHEN
18	4.845	naphthalene	128	PAH
19	5.115	propylcyanobenzene	91+131	NCOMP
20	5.193	4-vinylphenol	91+120	LIG
21	5.266	C ₃ -phenol	121+136	PHEN
22	5.739	indole	117+90	NCOMP
23	5.843	3-acetamido-5-methylfuran	97+(69+)+139	NCOMP
24	5.858	C ₁ -naphthalene	142+141(+115)	PAH
25	5.864	p-tert-butylphenol	135+107(+150)	cont
26	5.931	C _{3:1} phenol (isopropenyl?)	134+119	cont
27	5.994	C ₁ -naphthalene	142+141(+115)	PAH
28	6.139	3-acetamido-2/4-pyrone	111+(82+)+153	NCOMP
29	6.550	C ₁ -indole	130+131	NCOMP
30	6.566	biphenyl	154	PAH
31	8.214	fluorene	166+165	PAH
32	8.458	5-bromoindole	197+195(+116+89)	NCOMP
33	8.521	levoglucosan	60+73	CARB
34	8.988	diketodipyrrole	186+93	NCOMP
35	9.623	phenanthrene/anthracene	178	PAH
36	9.680	C ₁₄ -fatty acid	60+73	MCC
37	10.117	alkane/alkene pair	55+57	MCC

Continued on next page

Continued from previous page

Label	RT (min)	Compound	m/z	group
38	10.158	phenylnaphthalene	204+203	PAH
39	10.283	phytadiene 1	68+95(278)	MCC
40	10.496	diketopiperazine	70+154+194	NCOMP
41	10.507	C ₁₆ -alkylnitrile	97	NCOMP
42	10.579	phytadiene 2	81+82(278)	MCC
43	11.006	C ₁₆ -fatty acid	60+73	MCC
44	12.191	C ₁₆ -alkylamide	59+72	NCOMP
45	12.243	p,p'-isopropylidenebisphenol	213+228	cont
46	12.243	C ₁₈ -fatty acid	60+73	MCC
47	14.229	unknown compound	(91+129+207)	other
48	16.013	triterpenoid compound	368+353	other
49	16.663	triterpenoid compound	69+269(+298)	other